International Journal of Advanced Scientific Research
www.allscientificjournal.com
ISSN: 2456-0421
Received: 02-03-2026, Accepted: 01-04-2026, Published: 16-04-2026
Volume 11, Issue 2, 2026, Page No. 9-16

Pindiga bentonite clay adsorbent: Sustainable material for photocatalytic and phenol environmental remediation in Nigeria

Umudi Ese Queen[1], Umudi Ogheneyoma Peter[2]
[1] Department of Chemical Science, University of Delta, Agbor, Nigeria
[2] Department of Biotechnology, Delta State University, Abraka, Nigeria

Abstract
The potential of Pindiga bentonitic clay for phenol adsorption and photocatalytic degradation was explored. The clay was treated with oxalic acid and calcined at 1000°C, demonstrating effective phenol adsorption and degradation under visible light. Various analyses, including X-Ray Fluorescence (XRF), X-Ray Diffraction (XRD), and surface area measurements, were conducted. Acid-treated clays, especially those treated for 60 minutes (PB-60), exhibited higher surface areas (363.61 m^2/g) compared to raw (PB) and calcined (PBC) clays. Phenol adsorption kinetics were studied using pseudo-first and pseudo-second order models, with the data fitting the Freundlich model well, indicating heterogeneity in the adsorption sites. PB-60 exhibited the best monolayer coverage and phenol affinity. Adsorption efficiency decreased as pH rose from 5 to 11, with optimal adsorption occurring at lower pH values. Increased catalyst dosage also enhanced adsorption. For photocatalytic degradation, the Langmuir-Hinshelwood model was applied, with PB-60 showing superior degradation of phenol compared to PB, PBC, and PB-5 under visible light. The optimal catalyst dosage for photocatalysis was found to be 2.5g/l. The study highlights the potential of Pindiga bentonitic clay, particularly the PB-60 variant, as an effective adsorbent and photocatalyst for phenol removal from aqueous solutions.

Keywords: Pindiga bentonite clay, photocatalytic, phenol, adsorbent, remediation

Introduction

The development of advanced materials for environmental management has become a critical area of research due to the growing concerns over pollution and the depletion of natural resources. As industries and urbanization continue to expand, the need for sustainable methods to address environmental contamination, such as the removal of harmful pollutants from water and air, has gained significant attention (Umudi *et al*., 2025) [14]. Among the various techniques for pollutant removal, adsorption and photocatalysis are two of the most promising approaches. These methods offer an eco-friendly, cost-effective, and efficient means of cleaning the environment, particularly in addressing heavy metals, organic compounds, and other contaminants that pose serious risks to human health and the ecosystem. In recent years, there has been a strong focus on utilizing natural and abundant materials for developing adsorbents and photocatalysts (Obruche *et al*., 2019) [8]. Clay minerals, which are widely distributed in the Earth's crust, have emerged as viable candidates for such applications due to their unique physicochemical properties, such as high surface area, ion-exchange capacity, and structural stability (Itodo *et al*., 2021) [6]. Among the various types of clays, bentonitic clay has gained significant attention owing to its high adsorption capacity, availability, and relatively low cost. One such promising resource for adsorbent and photocatalyst development is Nigerian Pindiga bentonitic clay (Erienu *et al*., 2022) [4]. Found in the northeastern region of Nigeria, Pindiga bentonite possesses distinctive properties that make it a potentially valuable material for environmental remediation (Umudi *et al*., 2025) [15]. However, despite its abundant availability, there has been limited exploration of its full potential in the development of adsorbents and photocatalysts (Ekpo *et al*., 2023) [12]. This research aims to bridge this gap by investigating the modification of Pindiga bentonitic clay to enhance its properties for applications in adsorption and photocatalysis (Abeokuta *et al*., 2025) [1]. Specifically, the study will focus on optimizing the clay for the removal of contaminants such as heavy metals, organic pollutants, and dyes from wastewater and air, as well as evaluating its photocatalytic efficiency under various conditions (Obruche *et al*., 2018) [9]. By exploring the potential of Nigerian Pindiga bentonitic clay, this research will contribute to the advancement of sustainable and cost-effective materials for environmental remediation, providing a local solution to global pollution challenges.

Materials and method

Materials

The following is a list of materials: Bentonite clay sourced from Pindiga, Gombe State, along with Oxalic acid, Distilled water, Phenol, NaCl, KMnO4, HCl, and NaOH, were utilized throughout this study. All materials mentioned were procured from Jossy Chemical Stores located in Zaria, Nigeria, and were produced by BDH Chemicals in England. The chemicals used were of analytical grade.

Sample Collection

The methodology for sample collection, identification, and treatment was in accordance with the procedures established by Obruche *et al*. (2019) [10]. Bentonite clay was obtained from the Unenurhie community in the Ughelli North Local Government Area of Delta State. After collection, the samples were transported to the Chemistry Department at Delta State College of Education in Mosogar for identification.

Leaching of Pindiga Bentonite Clay Using Oxalic Acid Solutions

The sample preparation method was derived from the research conducted by Adefila *et al*. (2003) [2].

Leaching experiments were performed in a 1-liter round-bottom glass flask maintained at a temperature of 100°C. The flask, which was fitted with a thermometer and a reflux condenser, was heated using a thermostatically controlled heating mantle. Magnetic stirring was employed throughout the process. All leaching experiments were conducted at atmospheric pressure. For each experiment, 500 ml of a 0.5M oxalic acid solution ($C_2H_2O_4$, reagent grade) was introduced into the flask, and the temperature was maintained at 100°C. Subsequently, 5.0 g of clay was added to the flask while magnetic stirring continued. Following the designated leaching period, the slurry was filtered while hot using a vacuum filtration pump, then immediately centrifuged, and dried at 110°C for 24 hours. The dried residue was calcined at 1000°C for 4 hours to yield iron oxides in the hematite polymorph state (αFe_2O_3), which demonstrate the highest photocatalytic.

Adsorption Experiments

The adsorption experiment was carried out following the guidelines set forth by Rengaraj *et al*. (2002) [13]. Adsorption experiments were conducted by allowing a precisely measured quantity of either raw or leached bentonites to achieve equilibrium with phenol solutions of known concentrations. The initial phenol concentrations ranged from 62.5 to 500 mg/l. A total of 2.5 g of bentonite was introduced into conical flasks, each containing 100 ml of phenol solution. This mixture was continuously stirred using a magnetic stirrer for duration of up to ten hours, during which aliquots were collected at various time intervals, filtered, and subsequently analyzed using UV/Vis spectrophotometry.

Effect of pH

A precise 2.5 g of bentonite was added to a narrow-neck bottle containing 100 ml of a phenol solution at a concentration of 500 mg/l. The pH was adjusted with dilute solutions of HCl or NaOH. The pH values utilized were 5, 9, and 12. This mixture was stirred continuously with a magnetic stirrer for a period of 10 hours.

Effect of initial phenol concentration

Approximately 100 ml of initial phenol concentrations (62.5, 125, 250, and 500 mg/l) were combined with 2.5 g of bentonite in narrow-neck bottles, respectively, and stirred continuously in the dark for 12 hours.

Effect of adsorbent dose

A precise 100 ml of phenol was measured and placed in a beaker, to which 1.5 g of the catalyst was measured and added. The beaker was then placed on a hot plate, and a magnetic stirrer was introduced to continuously stir the contents in the dark for 10 hours, after which an aliquot was collected for analysis. This procedure was repeated for catalyst amounts of 2.0 g, 2.5 g, and 3.0 g.

Photocatalytic experiments

The photocatalytic method adhered to the protocol established by (Obruche *et al*., 2019) [10]. All photocatalytic experiments were executed following the same procedure. A stock solution with a concentration of 500 mg/l of phenol (the substrate) was prepared in deionized water for all experiments. A volume of 100 ml of this solution was placed in the reactor, to which 2.5 g of catalyst was added. The pH of the solution during dark adsorption was recorded. Subsequently, the suspension was subjected to irradiation from a 500W halogen lamp while being continuously stirred with a magnetic stirrer for a duration of two hours. At regular time intervals, aliquots were extracted from the reactor using a syringe. The catalyst was then separated from the sample through filter paper. These samples underwent analysis via a UV-Vis spectrophotometer. The pH of the final solution was also recorded. To ensure the reproducibility of the results, the experiments were conducted in duplicate. Various experiments were carried out to optimize parameters such as initial concentration, pH, and catalyst loading for the degradation of phenol using the aforementioned procedure. Prior to the photocatalytic treatment under optimized conditions, the phenol solution and catalyst were stirred continuously for six hours to establish adsorption-desorption equilibrium.

Determination of specific surface area of the clay

Determination of the specific surface area of the clay was conducted using methods similar to those outlined by Ekpo *et al*. (2025) [3], with minor modifications. In this approach, a constant relative humidity for the adsorbate was established, corresponding to the relative humidity of water vapor derived from a saturated salt solution in water. This relative humidity was confirmed to be equal to the following: First, two saturated solutions of four different types of salts were prepared. One solution of each salt was placed in a desiccator, while the other was left exposed in the laboratory. Both setups were allowed to sit for 24 hours, during which the initial and final weights were recorded. The relative humidity of the saturated salt solution for each salt was then calculated as the ratio of the weight differences of the salt solution in the desiccator (from the initial point to after 24 hours) to the weight differences of the salt solution left open (from the initial point to after 24 hours). The salts utilized in this study include $CaSO_4$, K_2SO_4, CH_3COONa, and $MgCl_2$. Following the determination of the value of to for each salt, a saturated solution of each salt was prepared and placed in a desiccator containing 1g of the adsorbent (synthesized catalyst) evenly distributed on a petri dish. This setup was maintained in conjunction with the saturated salt solution within the airtight desiccator for a duration of 24 hours, ensuring that the laboratory temperature remained at room temperature. At the conclusion of the 24-hour period, the weight gain of the catalyst was measured to represent v in equation 2.5. This procedure was subsequently repeated for the other catalysts, and equations (2.4 to 2.16) were employed to calculate the specific surface area of the synthesized catalyst (Adefila *et al*., 2003) [2].

Results and Discussion Leaching of Clay

Pindiga bentonite clay underwent treatment with a 0.5M oxalic acid solution at a temperature of 100°C, with leaching times varied at 0, 5, and 60 minutes. Both the raw and acid-leached clays were activated through calcination at 1000°C. The clays, both raw and treated, were designated according to their leaching times as PB (Raw Clay), PBC (Raw clay calcined at1000^{o}C), PB-5 (Raw clay treated for 5

mins with 0.5 M oxalic acid then calcined at1000ºC), and PB-60 (Raw clay treated for 60mins with 0.5 M oxalic acid then calcined at1000ºC)

Specific Surface Areas and Crystallite Sizes of the Untreated and Processed Clays

Appendices A and B provide a comprehensive description of the water adsorption technique employed to ascertain the surface area, along with Scherrer's equation utilized for calculating the particle sizes of PB, PBC, PB-5, and PB-60, respectively. Table 1 presents the specific surface areas and particle sizes as measured.

Table 1: Specific surface areas and particle sizes of PB, PBC, PB-5 and PB-60

Catalysts	Surface area(m^2/g)	Particle size(nm)
PB	47.13	14.76
PBC	151.69	65.84
PB-5	265.99	57.06
PB-60	363.61	51.25

The surface areas of both raw and treated clays are detailed in Table 1. Among these, PB-60 exhibits the largest surface area at 363.61 m^2/g, followed by PB-5 with a surface area of 265.99 m2/g, then PBC at 151.69 m^2/g, and finally PB with a surface area of 47.13 m^2/g. The superior surface area of PB-60 can be attributed to a longer leaching time with acid, which positively influences the surface area compared to the other catalysts (Obruche *et al*., 2025) [7]. Additionally, Table 1 provides information on the particle size of the clays.

Characterization of the Catalysts

Table 2 presents the X-ray fluorescence data for raw Pindiga clay alongside the developed catalysts, with their structures illustrated in Figure 1. The X-ray fluorescence (XRF) results in Table 2 indicate that Pindiga bentonite clay from Gombe State, Nigeria, contains a significant amount of iron oxide (26.24 wt. %), which serves as a key motivation for this research project. The X-ray diffraction (XRD) pattern depicted in Figure 1 reveals peaks corresponding to hematite, Ca-montmorillonite, and other significant peaks that align with standard peaks for bentonite clays. These analyses confirm that the clay is indeed a bentonitic type with additional compositions, consistent with typical XRF and XRD findings reported in the literature for bentonite clays (Ogwuche & Obruche, 2020) [11].

Table 2: Composition of the PB, PBC, PB-5, and PB-60

		Concentration (wt %)		
Component	**PB**	**PBC**	**PB-5**	**PB-60**
A2O3	14	15.94	16.8	17.6
SiO_2	43.6	47.66	56.1	57.3
K_2O	3.52	3.68	3.92	3.86
CaO	2.46	1.71	1.33	1.44
TiO_2	2.06	2.09	2.15	2.37
V2O5	N/A	0.15	0.11	0.11
Cr_2O_3	N/A	0.05	0.04	0.039
MnO	N/A	N/A	0.08	0.1
Fe_2O_3	26.54	21.47	17.33	15.71
NiO	N/A	N/A	0.01	0.06
CuO	N/A	0.03	0.03	N/A
ZnO	0.03	0.05	0.07	0.14
Ag_2O	N/A	3.4	2.46	2.8
BaO	N/A	N/A	0.22	0.26
SO_3	1	N/A	N/A	N/A
CaO	2.46	N/A	N/A	N/A
Eu_2O_3	N/A	N/A	0.19	0.16
Yb_2O_3	0.03	0.03	0.02	0.01
Re_2O_7	0.14	0.11	0.1	0.1

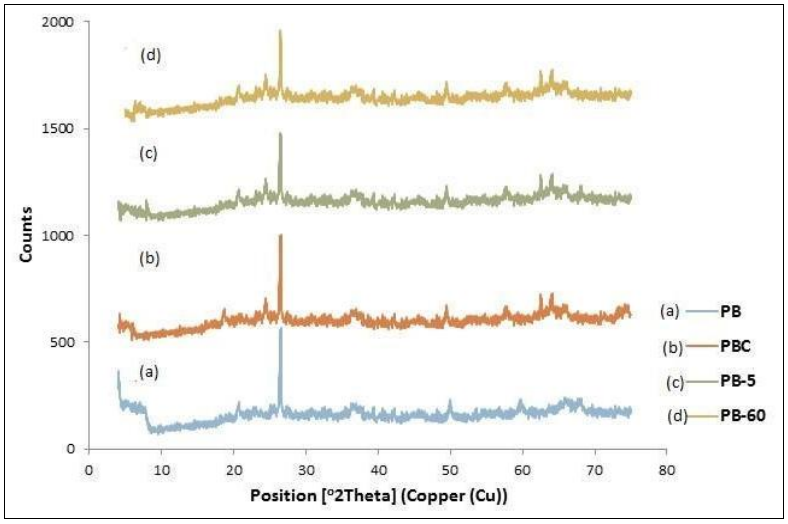

Fig 1: Cascaded XRD patterns of (a) PB, (b) PBC, (c) PB-5 and (d) PB-60

Preliminary Photocatalytic before Adsorption Equilibrium was Established

Degradation of Phenol Figure 2 shows the photocatalytic phenol degradation by various catalyst; PB, PBC, PB5 and PB-60. This experiment was carried out before adsorption equilibrium was established.

Figure 2 illustrates that PB exhibits a significantly low degradation capacity for phenol, achieving only 5% degradation within 2 hours. In contrast, PBC demonstrates improved photocatalytic activity at 25%, while PB-5 follows with a 30% degradation rate. The most effective photocatalyst, PB-60, successfully degrades phenol by 35% in the same time frame. Overall, the degradation performance of the clays is suboptimal. This may be attributed to the lack of established adsorption equilibrium prior to the initiation of photodegradation.

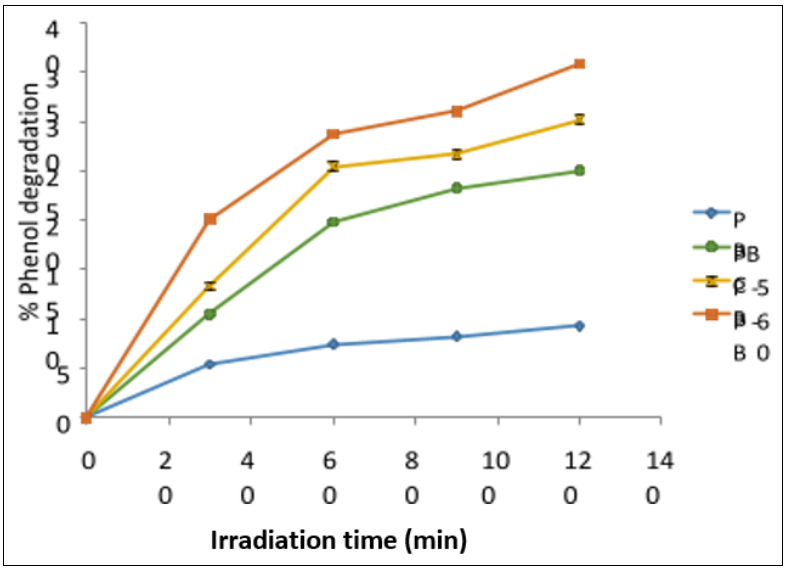

Fig 2: Effect of irradiation time on the photocatalytic degradation of phenol by PB, PBC, PB-5 and PB-60

Adsorption of Phenol on PB, PBC, PB-5 and PB-60

The adsorption data detailing the uptake of phenol in relation to contact time at various initial concentrations for PB, PBC, PB-5, and PB-60 is provided in Tables 3 – 6. The analysis of this data employed pseudo-first order kinetics, pseudo-second order kinetics, intraparticle diffusion, as well as the Langmuir and Freundlich adsorption models

Table 3: Concentration measurement for the adsorption of phenol by catalyst PB

		Concentration		
Ad. Time(hrs)	**500mg/l**	**250mg/l**	**125mg/l**	**62.5mg/l**
0	429.714	243.286	129.714	68.286
1	420.857	236.286	123.714	63.429
2	413.429	229.429	119.286	61.143
4	399.429	219.714	115.000	59.143
6	393.286	216.571	112.143	58.286
8	393.286	216.571	112.286	58.286
10	393.429	216.571	112.143	58.286

Table 4: Concentration measurement for the adsorption of phenol by catalyst PBC

		Concentration		
Ad. Time(hrs)	**500mg/l**	**250mg/l**	**125mg/l**	**62.5mg/l**
0	429.714	243.286	129.714	68.286
1	405.143	224.857	117.000	59.429
2	396.286	218.429	112.571	56.857
4	382.143	208.286	106.429	52.571
6	370.714	199.286	101.429	51.143
8	370.714	199.286	101.429	51.143
10	370.714	199.286	101.429	51.143

Table 5: Concentration measurement for the adsorption of phenol by catalyst PB-5

		Concentration		
Ad. Time(hrs)	**500mg/l**	**250mg/l**	**125mg/l**	**62.5mg/l**
0	429.714	243.286	129.714	68.286
1	376.571	206.857	102.714	52.000
2	359.143	193.571	96.857	49.286
4	334.000	181.857	92.143	45.857
6	322.571	173.571	86.286	43.571
8	322.571	173.571	86.286	43.571
10	322.571	173.571	86.286	43.571

Table 6 Concentration measurement for the adsorption of phenol by catalyst PB-60

		Concentration		
Ad. Time(hrs)	**500mg/l**	**250mg/l**	**125mg/l**	**62.5mg/l**
0	429.714	243.286	129.714	68.286
1	354.000	179.714	85.000	36.857
2	321.571	154.429	71.714	33.000
4	261.286	132.571	56.429	26.857
6	236.857	111.714	50.571	23.571
8	236.857	111.714	50.571	23.571
10	236.857	111.714	50.571	23.571

Table 3-6 illustrates that the duration necessary for the equilibrium adsorption of phenol onto the clays was six hours. The adsorption of phenol by the clays is observed to increase with a rise in the initial phenol concentration. An increase in the initial phenol concentration enhances the mass transfer driving force, thereby accelerating the rate at which phenol molecules migrate from the bulk solution to the surface of the particles. Consequently, this leads to an increase in phenol adsorption. However, on a relative scale, the percentage of phenol adsorption diminishes as the initial phenol concentration escalates (Umudi *et al*., 2015) [17].

Adsorption Dynamics

The influence of initial phenol concentration at varying levels of 500, 250, 125, and 62.5 mg/l on the kinetics was examined. The kinetics of adsorption, a fundamental analysis for determining adsorption efficiency, characterizes the rate of solute uptake, which subsequently influences the residence time of the adsorption process. As shown in Table 7, a plot of log (qe – qt) against time (t) yielded a linear correlation; thus, k1 and qe were derived from the slope and intercept of this plot, respectively. Additionally, from Table 7, the ratio t/qt was plotted against time (t), which also produced a linear relationship; qe and k2 were ascertained from the slope and intercept of this plot. A plot of qt against t1/2 was also created; in this case, the slope provided the rate constant, kid. These findings are summarized in Tables 7.

Table 7: presents the kinetic parameters for the adsorption of phenol by both raw and treated Pindiga clays at a phenol concentration of 500 mg/l.

		1st Order Kinetics				2nd Order Kinetics			Intra-Particle Diffusion	
Catalysts/Ads. parameters	**k1 (min^{-1})**	**q_{ee} (mg/g)**	**qem (mg/g)**	**R^2**	**k2 (g/mg.min)**	**q_{ee} (mg/g)**	**qem (mg/g)**	**R^2**	**kid (mg/g. min1/2)**	**R^2**
PB	0.451	1.457	1.653	0.966	0.097	1.457	2.268	0.930	0.787	0.990
PBC	0.478	2.360	2.375	0.990	0.177	2.360	2.908	0.989	0.980	0.993
PB-5	0.555	4.286	4.203	0.993	0.132	4.286	4.941	0.994	1.615	0.997
PB-60	0.570	7.714	8.537	0.998	0.060	7.714	10.94	0.987	3.733	0.997

The investigation into the adsorption kinetics of phenol absorption by PB, PBC, PB-5, and PB-60 was conducted for phenol concentrations of 500, 250, 125, and 62.5 mg/l, respectively. The data presented in Tables 7 suggest that the adsorption process adheres to the pseudo-first order kinetic model. At a phenol concentration of 500 mg/l, PB-60 exhibited the highest rate constant of k1= 0.570 min-1 according to the pseudo-first order model, followed by PB-5 (k1= 0.555 min-1), PBC (k1= 0.478 min-1), and PB (k1= 0.451 min-1). The kinetic model did not adequately describe the process using pseudo-second order kinetics. PB-60 also demonstrated a greater intraparticle diffusion constant kid of 3.733 mg/g.min1/2 compared to PB-5 (1.616 mg/g.min1/2), PBC (0.981 mg/g.min1/2), and PB (0.788 mg/g.min1/2). This same order was observed at phenol concentrations of 250, 125, and 62.5 mg/l, as illustrated in Table 7, respectively. Similar findings have been reported by Obruche *et al*. (2025) [7] and Umudi *et al*. (2025) [18].

Equilibrium Isotherm Studies

To assess the adsorption capacity of the adsorbents (PB, PBC, PB-5, and PB-60) for phenol removal, the adsorption data were evaluated using the Freundlich and Langmuir isotherm models, as presented in Table 8.

Table 8: Equilibrium isotherm parameters for the adsorption of phenol by the raw and acid treated clays

	Langmuir			Freundlich		
Catalyst/Adsorption Parameters	**K_L (g/l)**	**qo (mg/g)**	**R^2**	**K_f (mg/g)**	**1/n**	**R^2**
PB	0.00424	2.169	0.929	0.0328	0.696	0.945
PBC	0.00457	3.551	0.989	0.0553	0.663	0.982
PB-5	0.00594	5.587	0.996	0.0619	0.640	0.991
PB-60	0.00688	12.69	0.996	0.2006	0.614	0.999

The findings indicate that the adsorption of phenol onto PB, PBC, PB-5, and PB-60 is most accurately represented by the Freundlich adsorption isotherm, as evidenced by R2 values exceeding 92%. As illustrated in Table 8, the elevated Kf-value of PB-60 (0.2006 mg/g) signifies a stronger affinity for phenol in comparison to PB-5 (0.0619 mg/g), PBC (0.0553 mg/g), and PB (0.03228 mg/g). The adsorption intensity, represented by 1/n, was determined to be 0.614, 0.640, 0.663, and 0.696 for the catalysts PB-60, PB-5, PBC, and PB, respectively. It was noted that in this system, the n values fulfill the heterogeneity condition, specifically $0<1/n<1$. In the context of the Langmuir adsorption model,

the increased adsorption capacity (qo) for PB-60 (12.69 mg/g) suggests that the quantity of phenol per unit weight of sorbent required to establish a complete monolayer on the surface is greater than that for PB-5 (5.587 mg/g), PBC (3.551 mg/g), and PB (2.169 mg/g). A relatively low KL-value (<0.007) indicates minimal surface energy across all adsorbents, thereby suggesting a potentially stronger interaction between phenol and the sorbents. Indeed, relatively low to moderate KL-values have been documented in numerous sorbent-phenol systems, including those involving palm-seed-coat-activated-carbon, bentonite, and rice husk (Umudi *et al*., 2025) [14]. The KL-values for PB-60, PB-5, PBC, and PB are recorded as 0.00688 g/l, 0.00594 g/l, 0.00457 g/l, and 0.00424 g/l, respectively. PB-60 demonstrated a good fit with kinetic models and exhibited superior equilibrium isotherm parameters, thus it was selected for further investigation.

Effect of Adsorbent Dosage

Here, Table 9 provides details regarding the results obtained from the influence of adsorbent dosage.

Table 9: Percentage uptake of phenol by various dose of PB-60 at phenol concentration of 500mg/l

Adsorption Time(hrs)/Sorbent dose	1.5g	2.0g	2.5g	3.0g
0	0.000	0.000	0.000	0.000
1	7.547	13.697	17.620	25.332
2	17.453	20.080	25.166	30.386
4	24.302	32.380	39.195	44.415
6	32.713	38.830	44.880	49.202
8	32.713	38.830	44.880	49.202
10	32.713	38.830	44.880	49.202

Table 9 presents the details regarding the percentage uptake of phenol by varying doses of PB-60 at a phenol concentration of 500 mg/l. It illustrates the quantity of phenol eliminated as a function of the adsorbent dosage from the solution, maintained at neutral pH and at a phenol concentration of 500 mg/l. The dosage of PB-60 was adjusted from 1.5 g to 3.0 g and allowed to equilibrate for a duration of 10 hours. The percentage of phenol removal exhibited an increase corresponding to the rise in adsorbent dosage. This phenomenon can be explained by the enhanced surface area of the adsorbent and the availability of additional adsorption sites that result from the increased dosage of the adsorbent. Equilibrium was reached at 6 hours, indicating that no further adsorption occurred beyond this time frame.

Effect of Solution pH

The adsorption behavior of phenol by PB-60 was examined at pH levels of 5, 9, and 11, as detailed in Table 10.

Table 10: Percentage uptake of phenol at various pH values of PB-60 at phenol concentration of 500mg/*l*

Adsorption Time (hrs)/Solution pH	pH=5	pH=9	pH=11
0	0.0	0.0	0.0
1	25.9	22.9	20.7
2	29.3	25.1	23.4
4	32.7	29.0	27.0
6	39.6	35.4	29.6
8	39.6	35.4	29.6
10	39.6	35.4	29.6

The findings presented in Table 10 indicate that the quantity of adsorbed phenol diminishes as the pH value increases. This phenomenon can be explained by the relationship between phenol ionization and pH levels. Consequently, phenol, classified as a weak acid (pKa = 10), exhibits reduced adsorption at elevated pH values. A similar trend has been documented by Umudi *et al*.
(2025) [15] regarding the adsorption of phenol onto activated carbon.

Photocatalytic Degradation of Phenol Utilizing PB, PBC, PB-5, and PB-60

The kinetic degradation of phenol for PB, PBC, PB-5, and PB-60 was examined through the application of the Langmuir-Hinshelwood (L-H) kinetic model across various initial concentrations, with the results detailed in Table 11. The values of kr exceeded those of KLH for all catalysts, suggesting that phenol adsorption is the rate-limiting step in the process. A comparable observation was made in the photodecolorization of methyl orange using alpha-Fe_2O_3-supported HY photocatalysts (Ugochukwu *et al*., 2025) [16]. Among the catalysts, PB-60 demonstrated the best fit with the model and was therefore selected for further investigation.

Table 11: Derived Langmuir-Hinshelwood kinetic parameters.

Catalysts/kinetic parameters	kr (mgL-1min-1)	KLH (Lmg-1)	R^2
PB	0.3777	0.0353	0.954
PBC	0.4852	0.0353	0.980
PB-5	3.8314	0.0035	0.991
PB-60	6.8483	0.0034	0.999

Effect of pH

Lower pH values are observed to be favourable for the photocatalytic degradation of phenol by PB-60 as presented in Table 12. PB-60 was more efficient in photo degrading phenol at a pH of 5 as compare to a pH of 11.

Table 12: Effect of solution pH on the photocatalytic degradation of phenol by PB-60 at phenol concentration of 500mg/l

Kinetic parameter/pH values	pH=11	pH=9	pH=5
K (min^{-1})	0.0001	0.005	0.008
R^2	0.948	0.992	0.997

Effect of catalyst dosage

The catalyst dosages were varied from 1.5g to 3.0g and photodegradation of phenol was carried out for 2 hours as shown in table 12.

Table 13: Effect of catalyst dosage on the photocatalytic degradation of phenol withphenol concentration of 500mg/l by PB-60

Kinetic parameter /catalyst dose	1.5g	2.0g	2.5g	3.0g
Kapp (min-1)	0.002	0.003	0.007	0.005
R^2	0.91	0.964	0.999	0.999

The influence of photocatalyst concentration on the rate of phenol degradation has been examined by utilizing various concentrations of PB-60, ranging from 1.5 to 3.0 g/l, under visible light exposure. The findings are summarized in Table 13. It was noted that the initial degradation rate increases with a rise in PB-60 concentration, reaching a peak at 2.5 g/l, after which it declines. The optimal

concentration of PB-60 for phenol degradation is determined to be 2.5 g/l. This indicates that increasing the PB-60 concentration to 2.5 g/l enhances the degradation of phenol. However, any further increase beyond 2.5 g/l adversely affects the photocatalytic degradation efficiency. This phenomenon occurs because an increase in photocatalyst quantity can lead to a light screening effect, which diminishes the surface area of the photocatalyst that is exposed to light, thereby reducing photocatalytic efficiency (Festus-Amadi *et al*., 2021) [5].

Conclusions

The conclusions derived from this study are as follows: Adsorbents and photocatalysts were synthesized from Pindiga bentonitic clay through oxalic acid leaching and calcination at 1000°C for four hours. The catalysts' physicochemical properties were analyzed using XRF, XRD, and surface area analysis. PB-60 showed the highest surface area at 363.61 m2/g, followed by PB 5 with 265.99 m2/g, then catalyst PBC at 151.69 m2/g, and finally PB with 47.13 m2/g. The pseudo-first order kinetic model and intra-particle diffusion model provided a better fit for the adsorption data, while the pseudo-second order kinetic model did not correlate well. The equilibrium data in aqueous solutions was best explained by the Freundlich isotherm. An increase in pH was found to impede adsorption and photocatalytic processes. Better adsorption and photocatalysis occurred at a lower pH (acidic medium). The kinetics of phenol's photocatalytic degradation were accurately represented by the Langmuir-Hinshelwood kinetic model. The optimal catalyst dosage needed for photocatalytic degradation was 2.5 g/l.

References

1. Abeokuta OJ, Uriri SA, Obruche EK, Okurame O. Hydrochemical Assessment of Borehole Water Quality in Eku, Delta State, Nigeria. Journal of Science, Technology and Environmental Studies,2025:1(2):17-25.
2. Adefila SS, Aderemi BO, Ajayi OA, Bederin DA. Comparative Surface Area Determination Using Water Adsorption Method: Nigeria Journal of Engineering,2003:11(2):88-95.
3. Ekpo Ekokodu Rose, Erienu Obruche Kennedy, Abiye Clement Marcus. Spatial and Temporal Variations in the Concentrations of Polycyclic Aromatic Hydrocarbon, in Ambient Air From Three Different Locations in River State, Nigeria. International Journal of New Chemistry,2025:12(4):567-580.
4. Erienu Obruche Kennedy, Itodo Adams, Wuana Raymond, Sesugh Ande. Polycyclic Aromatic Hydrocarbons in Harvested Rainwater in Warri and Agbarho, Nigeria. Bulletin of chemical society of Ethiopia,2022:36(4):27-35.
5. Festus-Amadi IR, Erhabor OD, Ogwuche Christiana E, Obruche EK. Characterization of Contaminated Sediments Containing Polycyclic Hydrocarbons from Three Rivers in the Niger Delta Region of Nigeria. Chemistry Research Journal,2021:6(3):1-12.
6. Itodo AU, Wuana RA, Erhabor OD, Obruche EK, Agbendeh ZM. Evaluating the Effects of Roofing Materials on Physicochemical Properties of Harvested Rainwater in Warri, Delta State, Nigeria. Chemical Society of Nigeria Journal, Kano,2021:12(1):234-245.
7. Obruche EK, Emakunu SO, Ugochukwau GC. Rainwater Harvesting: Microbial and Chemical Water Quality Assessment in Warri District. Mosogar Journal of Science Education,2025:10(1):36-45.
8. Obruche EK, Erhabor OD, Itodo AU, Itopa ST. Spectrophotometric determination of iron in some commercial iron containinig tablets/capsule. International journal of advanced trends in computer applications,2019:1(1):231-235.
9. Obruche EK, Ogwuche CE, Erhabor OD, Mkurzurum C. Evaluation of the inhibitive effect of African Marigold (Tagetes erectal L.) Flower Extracts on the Corrosion of Aluminium in Hydrochloric Acid. International Journal of Advances in Scientific Research and Engineering,2018:4(12):167-177.
10. Obruche EK, Ogwuche CE, Erhabor OD, Mkurzurum C. Investigating Corrosion Inhibition Effects of Tagetes Erecta L. Leaf Extrac on Aluminium in Acidic Medium. Global Scientific Journals,2019:7(1):1-17.
11. Ogwuche CE, Obruche EK. Physio-chemical analysis of palm oils (elaeis guineensis) obtained from major markets in agbarho, unenurhie, opete, ughelli and evwreni town, Delta state, Nigeria. International journal of trend in scientific research and development,2020:4(2):56-60.
12. Ekpo RE, Marcus AC, Obruche EK. Spartial and Temporal Variations in the Concentration of Particulate Matter in Ambient Air from three Different Locations in River State, Nigeria. International Journal of Scientific Research in Chemical Science,2023:10(4):32-38.
13. Rengaraj S, Seuny-Hyeon M, Sivabalan R. Agricultural Solid Waste for the Removal of Organics: Adsorption of Phenol from Water and Wastewater by Palm Seed Coat Activated Carbon. Waste Management,2002:22:543-548.
14. Umudi EQ, Obruche EK, Sani MI, Onwugbuta GC, Aghemwenhio IS, Ikechukwu SC, *et al*. Evaluation of Polycyclic Aromatic Hydrocarbons (PAHs) Contents of Fishes, Waters and Sediments of Rivers Niger: Human Health Risk Assessment. Journal of Basics and Applied Sciences Research,2025:3(5):187-199. https://dx.doi.org/10.4314/jobasr.v3i5.20
15. Umudi Ese Queen, Ese Ekanem, Sani Mamman Ibrahim, Onwugbuta Godpower Chukwuemeka, Suleiman Abdulmajid, Magashi Luper, *et al*. Degradation Efficiencies of the Total Petroleum Hydrocarbons (TPHs) in the Soil Amended with Palm Bunch Ash and Tween 80 in Ibenomo L.G.A, Akwa Ibom State. International Journal of Chemistry and Chemical Processes,2025:11(5):1-20.
16. Ugochukwu Gladys Chioma, Ataine Theresa Ifeyinwa, Erienu Kennedy Obruche. Determination of the Physicochemical Properties of Soil Amended with Cassava Mill Effluent in Mosogar Area of Delta State. Mosogar Journal of Science Education,2025:10(1):81-89.
17. Umudi Ese Queen, Odontimi Nimighaye, Sani Mamman Ibrahim, Chidi Henry, Onwugbuta Godpower Chukwuemeka, Odejobi BabajideMichael, *et al*. Assessment of the Seasonal Variations in Heavy Metals Concentration in the Ughelli Central Market River, Delta State, Nigeria. International Journal of Applied

Science and Mathematical Theory,2025:11(6):78-88. https//doi.org/10.56201/ijasmt.vol.11.no6.2025.pg78.88
18. Umudi Ese Queen, Ese Ekanem, Idongesit O. Ekpenyong, Sani Mamman Ibrahim, Onwugbuta Godpower Chukwuemeka, Suleiman Abdulmajid, *et al*. Seasonal Assessment of Heavy Metals Concentrations in Sediment of the Sapele River, Nigeria Journal of Science Innovation & Technology Research,2025:9(9):124–139.